ACS Sustainable Chemistry & Engineering

Research Article

pubs.acs.org/journal/ascecg

Aegle marmelos Leaf Extract and Plant Surfactants Mediated Green Synthesis of Au and Ag Nanoparticles by Optimizing Process Parameters Using Taguchi Method

K. Jagajjanani Rao and Santanu Paria*

Interfaces and Nanomaterials Laboratory, Department of Chemical Engineering, National Institute of Technology, Rourkela 769 008, Orissa, India

Supporting Information

ABSTRACT: The Taguchi method was used to optimize the phytochemicals mediated green synthesis parameters of silver (Ag) and gold (Au) nanoparticles. The ratio of respective metal ion precursor to *Aegle marmelos* leaf extract, plant based surfactants (Reetha, Acacia, and Shikakai), pH, temperature, and color of the light source were chosen as significant parameters affecting the size of the nanoparticles. The Ag (~13 nm) and Au (~23 nm) nanoparticles with narrow size distributions were produced after optimization of process parameters by the Taguchi method. Statistical analysis based on experimental results indicates that the pH and temperature have greater influence on the Ag nanoparticles size, whereas it is surfactant media and temperature for the Au nanoparticles. The square plate type nanoplates of Au with edge length of ~630 nm and width ~45 nm were also obtained by just changing the process parameters. This study shows the suitability of the Taguchi methodology in green synthesis and obtaining desired size nanoparticles for simple, one-pot, economical, and large scale production.

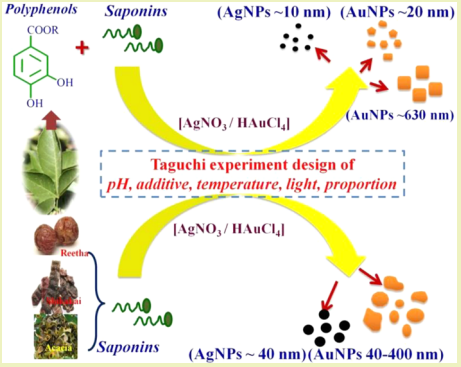

KEYWORDS: *Phytochemicals, nanoplates, Saponin, Reetha, Acacia, Shikakai*

INTRODUCTION

The noble metal nanoparticles (NPs) are well-known for their unique electronic, catalytic, and optical properties. Among different noble metals, Au and Ag possess various technological applications in the fields of optics, electronics, medical diagnostics and treatments, sensors, antimicrobial agents, coatings, etc.[1,2] Therefore, development of new methods ranges from chemical to biobased approaches for synthesizing smaller sized particles still have significant practical importance. In the case of a wet chemical process of NPs synthesis, the volume free energy is the driving force and surface free energy is the opposing force, as a result, the final particle size depends on the overall free energy of the system, which in turn again depends on the external parameters. So, the optimization of parameters is very important to get smaller sized NPs.

In spite of the fact that biobased approaches have gained more importance in the recent years with key advantages such as the eco-friendliness of the process and more biocompatible final products,[1,3] the optimization of process parameters for getting lower sized particles has been comparatively less focused. Among the biobased green synthesis methods of NPs, phytochemicals based methods are widely studied because of the ease and eco-friendliness of the process.[4−7]

In general, for handling of multiple parameters, all parameters of interest are used to be varied over a specified range in the form of a well-planned set of experiments to obtain systematic data. The method is popularly known as the factorial design of experiments or Taguchi method.[8] The basic principle of this procedure is to inspect the effects of experimental variables on the synthetic process using orthogonal arrays to design a minimum number of experiments. Here the design of experiments includes the study of any given system by a set of independent variables (factors) over a specific region of interest (levels).

The use of the Taguchi method also helps to optimize the parameters of NPs synthesis.[9−11] The method is used extensively for many chemical reactions, separation, and biochemical processes, compared to that of NPs synthesis. For the synthesis of SiO_2 and TiO_2 NPs via sol−gel process, this method was reported to design the right experimental parameters to get small sized particles.[9,10] Similarly, smaller sized silver chromate NPs (~75 nm) were also reported by optimizing the process parameters by the Taguchi method.[11]

The purpose of this study is to screen the key parameters for the green synthesis of smaller sized Ag and Au NPs. Optimization is a prerequisite for the large scale production of NPs to get smaller size particles as well as to minimize the use of excess reactants and experimental trials. In this regard,

Received: November 14, 2014
Revised: January 22, 2015
Published: January 30, 2015

DOI: 10.1021/acssuschemeng.5b00022
ACS Sustainable Chem. Eng. 2015, 3, 483−491

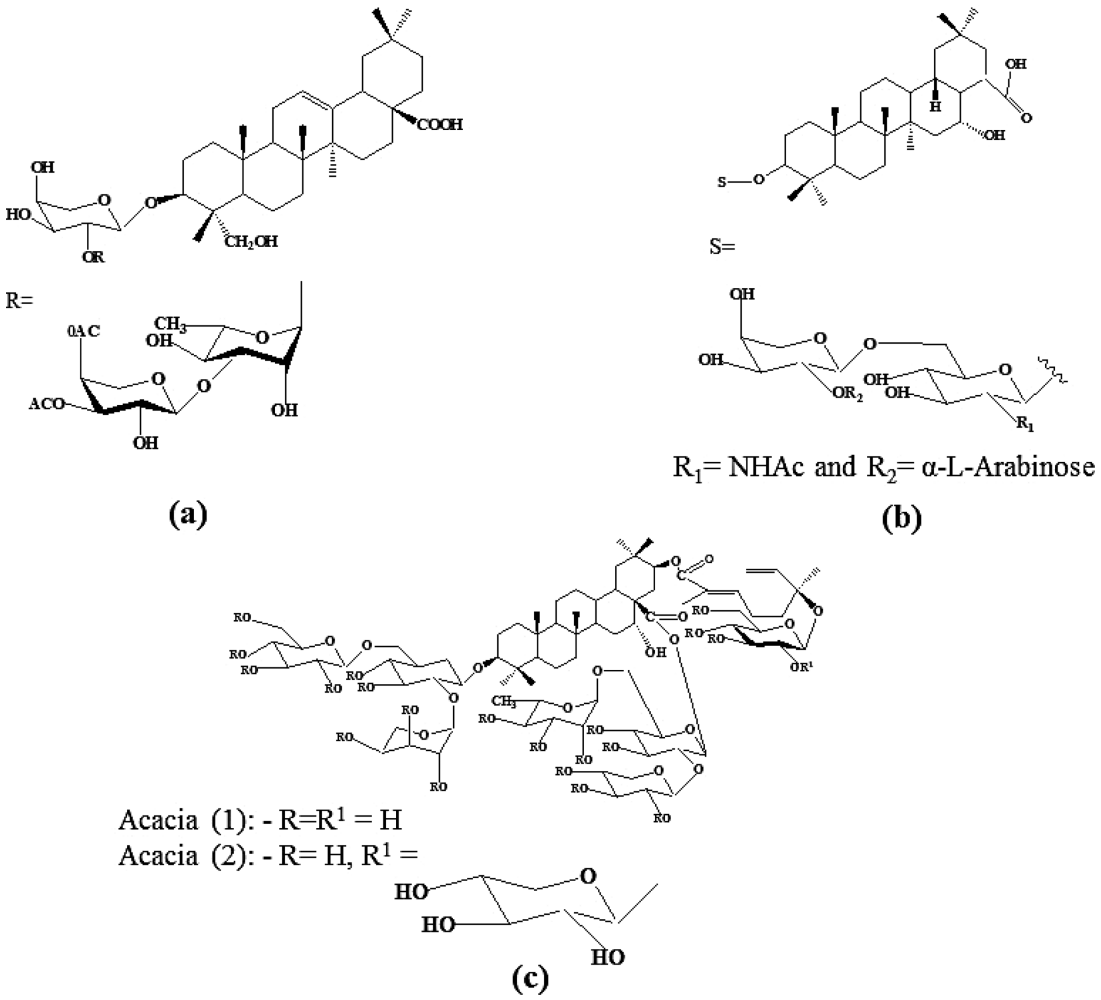

Figure 1. Structures of three plant surfactants (saponins) used in the study: (a) Reetha,[14] (b) Shikakai,[15,16] and (c) Acacia.[17,18]

one variable at a time was preferred generally by researchers from the conventional times to study the effect of various parameters. Because of many parameters, interrelationships with parameters, the overall study becomes complex, time-consuming, and trial-intensive. A simple and powerful design method like Taguchi can be used for increased productivity and performance of the process.[9−12]

Herein, we report the effects of pH, natural surfactants or saponins (Acacia, Reetha, Shikakai), temperature, light wavelength, and reactant proportions on the size and shape of Au and Ag NPs. The results of this investigation showed that Ag and Au NPs of various anisotropic shapes could be synthesized by selecting specific experimental conditions or by tuning significant parameters from primary results of orthogonal array. Once the key parameters affecting the synthesis procedure has been established, NPs with smaller or bigger sizes can be synthesized (based on the extinction spectra) by varying the levels of the significant parameters. Although various shape NPs are important, smaller size particles with narrow size distribution are also essential from the application perspective. Thus, optimal conditions for the synthesis of NPs were determined by Taguchi method. This approach via green procedure has not been used before to obtain smaller sized as well as different shapes Ag and Au NPs, employing *Aegle marmelos* with limited experimentations. In addition to the above, the obtained metallic NPs were tested for the antimicrobial activity against a model Gram-negative *Escherichia coli* bacterium also.

EXPERIMENTAL SECTION

Materials. The chemicals were purchased from the following companies: silver nitrate ($AgNO_3$), sodium bicarbonate ($NaHCO_3$), and acetic acid from Merck; chloroauric acid ($HAuCl_4$) of 49% Au from Loba Chemie. All chemicals used in this study were of analytical grade and were used as received without further purifications. Ultrapure water of 18.2 mΩ resistivity was used throughout the study.

Preparation of Leaf Extract and Saponins. A 5% stock solution of *Aegle marmelos* leaf extract (LE) was prepared as described in our previous study,[7] 30 mM stock solutions of Acacia (*Acacia auriculiformis*), Reetha (*Sapindus mukorossi*), and Shikakai (*Acacia concinna*) were prepared from vacuum-dried solid powders, obtained from their respective alcohol extracts. The method of preparation and purification was detailed in our previous studies as that of Reetha[13,14] and detailed in brief in SI-I (Supporting Information). The structures of three plant saponins are given in Figure 1.

Synthesis of Nanoparticles, Experimental Design, and Statistical Analysis. For the synthesis of NPs, various concentrations of LE were exposed to 1 mM $AgNO_3$/ $HAuCl_4$ to obtain the respective NPs. The Taguchi method[8] was used for the optimization of parameters to attain the possible smaller size Au and Ag NPs. Optimization of five key parameters such as pH, meida (presence of saponin), temperature, light wavelength (color of the light source), and reactant proportion [$AgNO_3$ or $HAuCl_4$ (mM)/LE (%)] in four different levels were studied, as shown in Table 1. Experiments were performed using L16 orthogonal array to synthesize individual Ag and

DOI: 10.1021/acssuschemeng.5b00022
ACS Sustainable Chem. Eng. 2015, 3, 483−491

Table 1. Parameters and Their Levels Used by the Taguchi Method for the Synthesis of Ag and Au NPs

parameter		level 1	level 2	level 3	level 4
pH		5.0	6.0	7.0	8.5
media[a]		water	Acacia	Reetha	Shikakai
temperature		10 °C	25 °C	40 °C	55 °C
light[b]		dark	white	blue	red
proportion	$AgNO_3$/LE	1/0.3	1/1.5	1/0.5	1/1.0
	$HAuCl_4$/LE	1/0.5	1/1.0	1/0.3	1/1.5

[a]The concentrations of 1.1 times CMC of Acacia, Reetha, Shikakai are 0.428, 0.564, and 0.55 mM, respectively. [b]Indicate the filter color used in the study.

Au NPs (Tables S1 and S2, Supporting Information) at various conditions. The responses were observed by UV−visible spectroscopy, considering the extinction spectra with wavelength maximum (λ_{max}) because of NPs formation, which in turn depend on the size and shape of the NPs.

Based on the results, a verification test was performed to check the optimized conditions. Analysis of variance (ANOVA) for the obtained results was also investigated. For the experimental design, ANOVA and the optimization of processes, MNITAB Release 14 (Minitab Inc., USA) was used.

Antimicrobial Studies. The antimicrobial activity of Ag and Au NPs were studied against *Escherichia coli* (NCIM 5051) by a zone of inhibition (ZOI) method.[19,20] The nutrient agar (NA) medium was used throughout the study for the growth of bacterium and overnight grown culture was used for the experimentation. A 40 μL of bacterial culture was spread on respective Petri plates with NA, and then wells of 4 mm were made on each plate. Further, 20 μL of 0.5 mM Ag and Au NPs were added into each well and incubated at 37 °C for 24 h. The ZOI was measured excluding the diameter of the agar well.

The structural changes of the bacterial surface in the presence of NPs were observed under scanning electron microscopy (SEM). For this, a 10 μL *E. coli* culture from 2% w/v was added to 1 mL of 0.5 mM individual NPs suspension in aqueous media, and the solution was incubated as stated above.

Analytical Methods. The UV−visible spectra of Ag and Au NPs were recorded using a spectrophotometer (UV-3600, Shimadzu). The structure and composition of the NPs were analyzed by high-resolution transmission electron microscopy (HR-TEM, JEOL-2100F) coupled with energy dispersive X-ray spectroscopy (EDS). The X-ray diffraction (XRD) measurements were done using Philips (PW1830 HT) X-ray diffractometer, in the range of 20−90° (2θ) at 0.05°/s scanning speed. Fourier transform infrared (FT-IR) spectroscopy (Thermo Fisher Scientific, Nicolet iS10) was done to identify the functional groups. The zeta (ζ) potentials were measured using a Malvern zeta size analyzer (Nano ZS, UK).

RESULTS AND DISCUSSION

Experimental Design by Taguchi Method. In general, synthesis methods of NPs are complex in nature and highly depend on more than one parameter. When the desired particle size is very small, fine controls of parameters are extremely important. The use of an optimization technique can help to get the optimum condition when more than one parameter is varying. The Taguchi method may be used quite easily because it has the ability to include categorical factors along with continuous ones. As the color of light (termed as "light" henceforth) has some role in the metal NPs synthesis such as Ag,[21,22] it has been studied as a categorical factor in this study to know its effect on Ag and Au NPs synthesis. Effects of pH, surfactant (media), temperature, and reactant proportion ($AgNO_3$/LE) were studied using L16 orthogonal array of Taguchi method. The experimental results for the synthesis of Ag and Au NPs in this section are tabulated in Tables S1 and S2 of the Supporting Information. The results are presented in terms of the maximum intensity values (λ_{max}) of UV−vis spectra because of surface plasmon resonance (SPR). The metal NPs, especially Ag and Au has strong interaction with light because of the presence of conduction electrons. When the electrons are excited by light of a specific wavelength, undergo a collective oscillation. This oscillation is known as SPR and this property can be utilized to fabricate new generation optical and sensor devices.[23] Thus, the λ_{max} values were monitored to get the smaller sized particles, which is very simple from the experimental perspective also.

The highest λ_{max} for Ag NPs was obtained from trial 10 (Table S1, Supporting Information) with the following experimental conditions: solution pH = 7.0, Acacia media, 55 °C, blue light, and $AgNO_3$/LE = 1/0.3. The highest λ_{max} value for Au NPs was from trial 7 (Table S2, Supporting Information) with experimental conditions: solution pH = 6.0, Reetha media, 55 °C, dark, and $HAuCl_4$/LE = 1/1.0.

It is important to note that the observed higher experimental λ_{max} values from the extinction spectra of Ag and Au NPs from various combinations of parameters were taken from L16 array without optimization. Upon critical evaluation of the main effects of the used parameters, one can have the right combination of key parameters with specific values or levels for high or low λ_{max} values from the extinction spectra. As our intention is to achieve the smaller size Ag and Au NPs, higher λ_{max} values from average of obtained results at various levels of factors are selected to depict the main effect of each factors or parameters. Figure 2a,b depicts the main effect of each of the studied factors. The term "main effect" depicts the average of the obtained results (of respective λ_{max}) in which each factor is at a given level. Dotted lines presented in Figure 2a,b indicate the average λ_{max} values from all the 16 experimental trials of Table S1 and S2 (Supporting Information). The resultant color

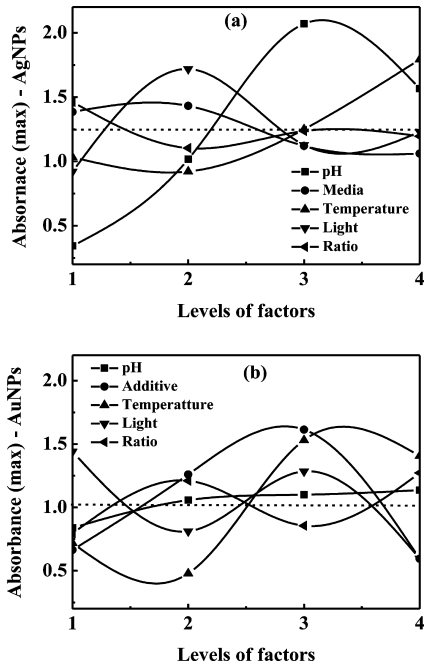

Figure 2. Main effects of factors or the average of the obtained results (of respective λ_{max}) for Ag (a) and Au NPs (b), in which each factor is at a given level. For a description of "levels", refer to Table 1.

DOI: 10.1021/acssuschemeng.5b00022
ACS Sustainable Chem. Eng. 2015, 3, 483−491

changes because of the formation of Ag and Au NPs are shown in Figure S1 (Supporting Information).

ANOVA results for the synthesis of Ag NPs are presented in Table S3 (Supporting Information) show that the change in pH of the synthesis media is the most important factor (with p-value 0.014 significant at the 0.05 α-level) followed by temperature (with p-value 0.08 significant at the 0.10 α-level). ANOVA of the main effects of factors for the synthesis of Au NPs (Table S4, Supporting Information) show that a change in temperature and media significantly affect the results (p-values are 0.027 and 0.031, respectively, significant at the 0.05 α-level). Further, the light is the moderately effective parameter (p-value 0.054 significant at the 0.10 α-level) for Au NPs synthesis, as presented in Table S4 (Supporting Information). The parameters with p-values > 0.1 from Tables S3 and S4 (Supporting Information) indicate the least importance on the synthesis process of individual Au and Ag NPs. In this study of the Ag and Au NPs synthesis process, factors for ANOVA are selected based on the higher R^2 value of the "estimated model coefficients for means" (refer to Tables S3 and S4, Supporting Information). Here, the R^2 value can explain variation in the responses of the model more adequately. The R^2 values are 0.973 (for Ag NPs) and 0.976 (for Au NPs) from the estimated model coefficients for means and by the parameter responses. This indicates that the Ag and Au NPs synthesis models are good fits and can explain >97% variation in the response.

Finally, after analyzing all results, the optimum conditions for getting intense extinction spectra with higher λ_{max} value for Ag and Au NPs are summarized and presented in Table 2. The

Table 2. Optimum Conditions Suggested for the Synthesis of Ag and Au NPs by Statistical Calculations after Performing the Tests

	Ag NPs			Au NPs		
parameter	parameter description	level	λ_{max} #	parameter description	level	λ_{max}
pH	7	3	0.82	8.5	4	0.10
media	Acacia	2	0.18	Reetha	3	0.58
temperature (°C)	55	4	0.54	40	3	0.50
light	white	2	0.47	dark	1	0.25
proportion	1/0.3	1	0.21	1/1.0	4	0.24
total contribution of all factors			2.23			1.67
current grand average of performance			1.25			1.03
expected result at optimum condition			3.47			2.7
obtained values			3.35			2.62

predicted SPR absorption intensities are 3.47 and 2.7 for Ag and Au NPs, respectively. To verify the calculated values, experiments were performed using these conditions and it can be seen that the experimental results are very close to that of predicted one. The obtained SPR intensities are 3.35 (448 nm) and 2.62 (600 nm) for Ag and Au NPs respectively as shown in Figure 3. The obtained values are 2.68 and 2.53 times more than the maximum average intensity values of Ag and Au NPs from Tables S1 and S2 (Supporting Information), and are 3.5% and 2.6% less than the predicted values for Ag and Au NPs, respectively. The differences between predicted and actual results are minimum (below 5%) and thus our results can be

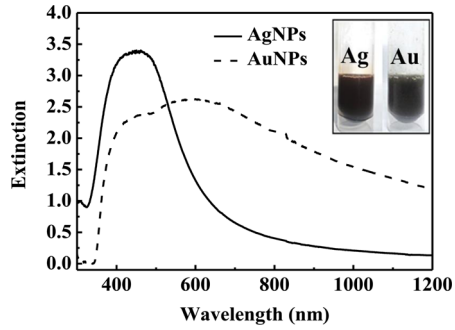

Figure 3. UV−visible-NIR spectra of the Ag and Au NPs synthesized from predicted optimum conditions upon dilution of 3.5 times. Inset shows the coloration due to formation of Ag and Au NPs.

acceptable.[24] The resultant Ag NPs formed after optimization of key parameters displayed a narrow SPR spectral pattern, while Au NPs exhibted a broad spectral pattern extended toward the red region of the visible wavelength to NIR region (Figure 3).

Further, the significance of the key parameters optimization and flexibility of the model was assessed by particle size and shape analysis of paramount results (with high λ_{max} values) of experiments from Tables S1 and S2 (Supporting Information) for Ag and Au NPs by atomic force microscopy (AFM). Figure 4 shows the size and morphologies of the experimental trials 10, 13, 11, and 9 for Ag NPs and trials with 7, 14, and 3 for Au NPs. The particle sizes from these experiments are comparatively higher and are not nearly uniform when compared with the Ag and Au NPs formed from parameters of optimized conditions (Figure 5). While analyzed the morphologies of the Ag NPs particles of different trials (trials 10, 13, 11, 9) and compared with their individual extinction spectra, one can notice two major changes. (i) Particle sizes are in wide range with a decrease in λ_{max} value, and (ii) prismatic structures are evident along with near spherical NPs with the increased tail broadening of the extinction spectra (Figure S1, Supporting Information). More prominent prismatic Ag structures were noticed from trial no. 9, compared to that of trial no. 11. Furthermore, analysis of particle morphology and their extinction spectra pattern of the best three Au trials (nos. 7, 14, and 3) with high λ_{max} values infers the following: (i) broad tail of the extinction spectrum from trial no. 14 compared to that of trial no. 7 and resulted in more anisotropic shapes of Au NPs, (ii) narrow extinction spectrum of Au NPs of trial no. 3 with two peak bands (one in visible and other in NIR region) resulted with limited anisotropic forms like square, triangular, and near spherical structures. Au NPs from this particular trial are detailed later in the Synthesis of Anisotropic Au Square Nanoplates section.

Conferring to the findings mentioned here, each experimental case with specific parameter values of L16 array of Taguchi method will give different size/shape NPs (as the extinction spectra of each trial is different) and can be selected according to the need after the analysis of particle morphology. However, smaller sized metal NPs with narrow size distribution is a necessity for a successful green route synthesis and application perspective.[25,26] Henceforth, smaller size Ag and Au NPs were successfully produced by optimization of key synthesis parameters by Taguchi method and are focused in the coming sections.

DOI: 10.1021/acssuschemeng.5b00022
ACS Sustainable Chem. Eng. 2015, 3, 483−491

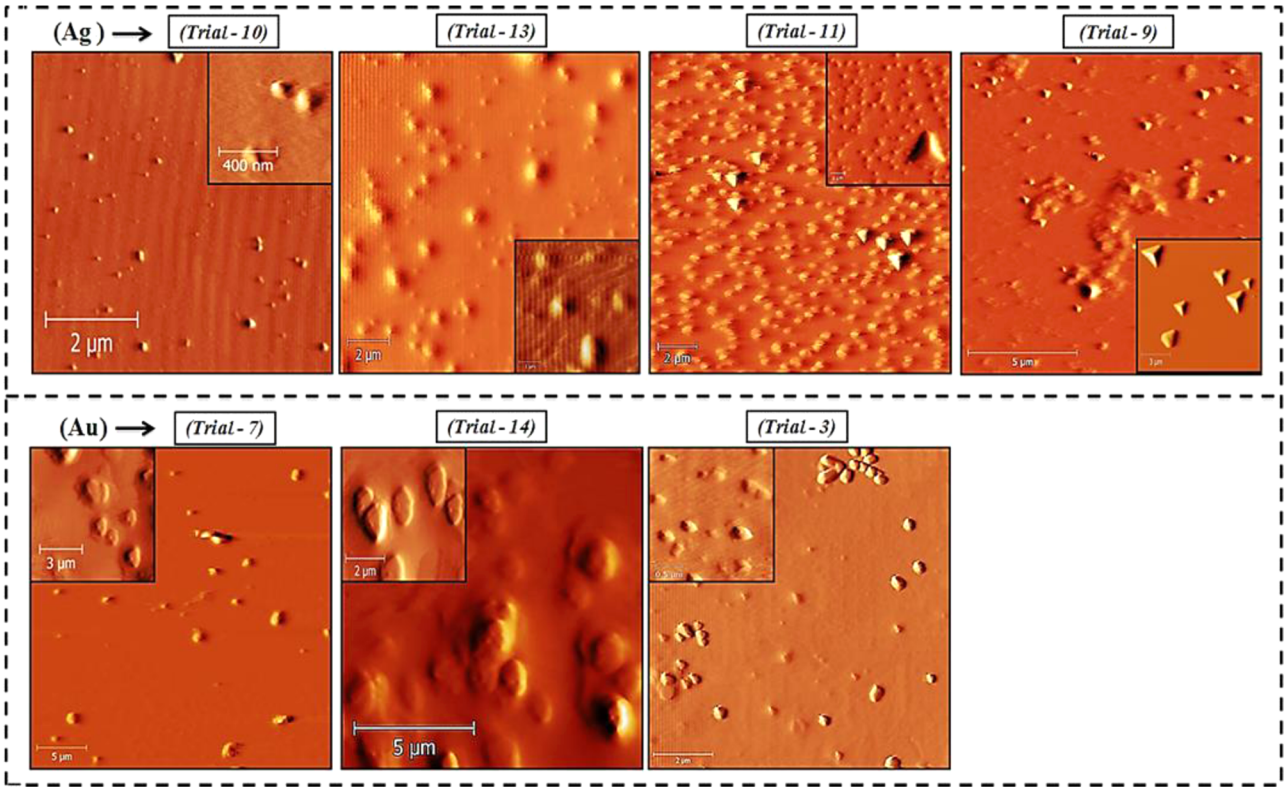

Figure 4. AFM images of Ag NPs (from trials 10, 13, 11, and 9) and Au NPs (from trials 7, 14, and 3).

Particles Characterizations (TEM, XRD, and ζ-Potential) from Optimum Conditions. Figure 5(a–d) and (e–h) shows the TEM images of Ag and Au NPs respectively synthesized using optimum conditions of various parameters shown in Table 2. Figure 5a–c suggests that the formed Ag NPs are mostly spherical structure. A TEM EDS spectrum of the figured particles is shown in Figure 5d, which confirms the presence of silver. The average particle size from the images was found to be ~13.83 ± 4.89 nm with narrow size deviations, as shown in the inset of Figure 5d.

A similar morphological analysis for Au NPs reveals an interesting result. Figure 5e–h shows the particle sizes are small and the shapes obtained are not uniform with significant variations. The shapes of the Au NPs from Figure 5e–h are near spherical, pentagons, smooth edged cubes, cuboids, etc. The magnified images of the pentagonal and hexagonal structures of Au NPs are shown in Figure 5f (inset), and near spherical, smooth edged cube and cuboid structures are evident in Figure 5g. Furthermore, the TEM EDS analysis clearly shows the presence of gold in Figure 5h. The average particle size of Au NPs with various shapes was found to be ~23 nm with reasonably narrow standard deviations as shown in Figure 5h (inset). The particle morphology observed from the TEM analysis supports our UV–vis-NIR results.

The XRD patterns of the Ag and Au NPs obtained from the optimum conditions (Table 2) are shown in Figure S2 in the Supporting Information. A number of Bragg reflections corresponding to (111), (200), (220), and (311) sets of lattice planes are observed and may be indexed based on the face centered cubic (fcc) structures of silver and gold. The diffraction patterns of Au matches with JCPDS file No: 04-0784 and that of Ag matches with JCPDS file No: 04-0783, which shows their high crystalline nature.

Further, the values of ζ potential of Ag and Au NPs from optimum conditions are also analyzed to see the capping effect of natural molecules on the particle surface. Figure S3 of the Supporting Information shows the ζ potentials of as-synthesized, water washed, and methanol washed Ag (from LE+Acacia) and Au NPs (from LE+Reetha). From Figure S3 (Supporting Information), it can be seen that a similar trend is followed by both Ag and Au NPs with negative ζ potential values when subjected to different washing steps. The ζ potential values are −14.35 ± 0.35, −20.85 ± 0.63, and −22.85 ± 0.21 mV for Ag NPs and −13.85 ± 0.21, −19.80 ± 0.42, and −22.35 ± 0.20 mV for Au NPs for as-synthesized, water wash, and methanol wash, respectively. As-synthesized NPs (Figure S3, Supporting Information) display, low ζ potential values because of adsorption or capping of natural molecules onto the particle surface. The ζ potential values increase for both particles after frequent water washing indicate partial removal of capped molecules. Further, the values obtained from methanol wash for Ag and Au NPs are close to the reported values (~−22.5 mV for Ag and −22 mV for Au)[7,27] of pure NPs. This confirms methanol wash can remove the adsorbed LE as well as the used natural surfactants (Acacia and Reetha) that cannot be removed easily by water wash alone.

Importance of LE and Surfactants on Particle Size. The NPs formation in control experiments devoid of LE with the conditions stated in Table 2 was also performed to know the ability of the used surfactant additives (Acacia and Reetha) on silver and gold metal ion reduction. Apart from surface active properties, the introduction of natural surfactants like saponins instead of synthetic surfactants enhances the process novelty and application prospects of the capped NPs. It has been also reported that the plant based saponins are natural antioxidants and are therapeutically effective toward a varieties

DOI: 10.1021/acssuschemeng.5b00022
ACS Sustainable Chem. Eng. 2015, 3, 483–491

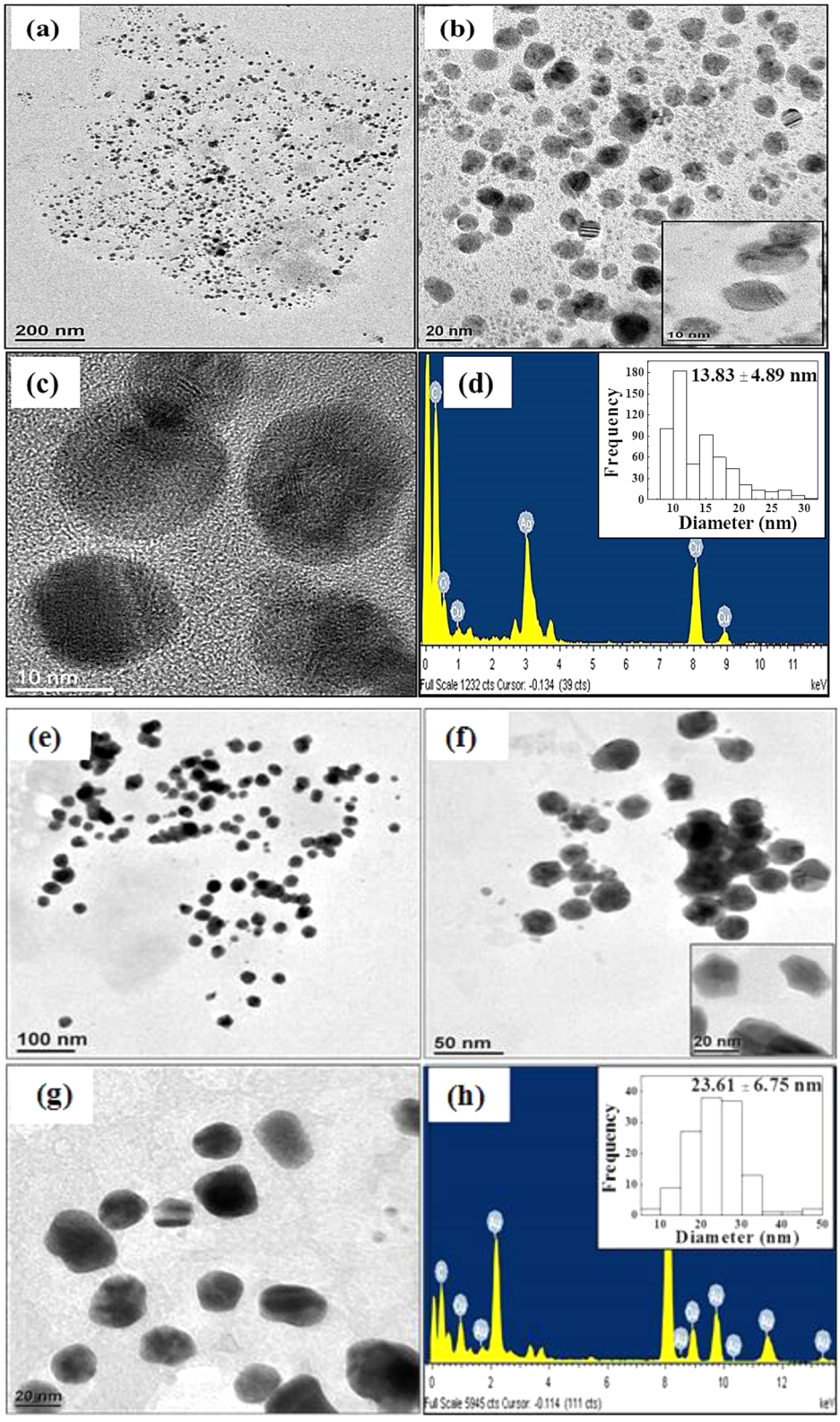

Figure 5. HR-TEM images of Ag (a–d) and Au (e–h) NPs at different magnifications along with EDS spectra. Particle histograms of the imaged particles are given in the respective insets.

of diseases including cancer and aging.[28] Recent studies supported that saponins can be conjugated with nanoparticles like platinum or Chitosan which has huge scope for biomedical applications.[28,29] Saponin's presence in aqueous extracts alone was also utilized for the mass production of Ag and Au NPs in a few studies.[28,29] Thus, expecting better size regulation, instead of synthetic surfactants, natural surfactants are chosen in this study, which may also be useful for different applications. The presence of the sugar derivatives (glycone moiety) of the saponins plays a key role in the reduction process. The exposed

DOI: 10.1021/acssuschemeng.5b00022
ACS Sustainable Chem. Eng. 2015, 3, 483–491

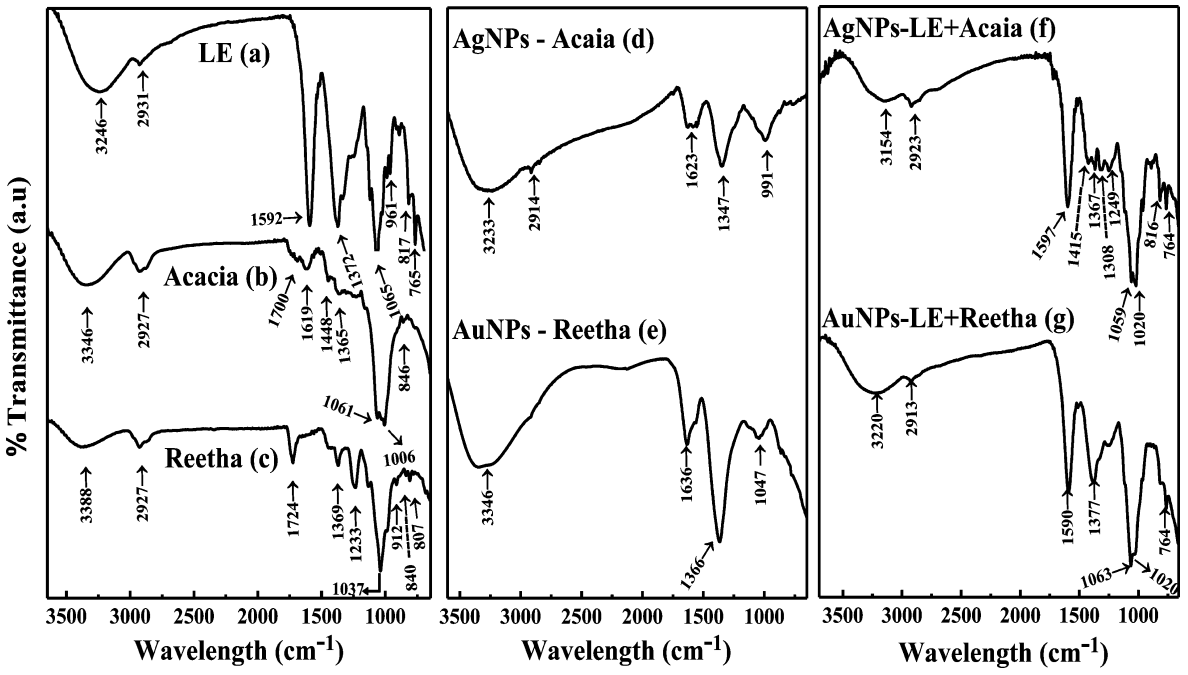

Figure 6. FT-IR spectra of pure extracts: (a) LE, (b) Acacia, and (c) Reetha. FT-IR spectra of water washed NPs are as follows: (d) Ag NPs synthesized from Acacia, (e) Au NPs synthesized from Reetha, (f) Ag NPs from LE+Acacia, and (g) Au NPs from LE+Reetha.

aldehyde groups of the glycone moiety in aqueous medium reduce the added metal precursor to metal NPs as follows

$$RCHO(aq) + OH^- \rightarrow RCOO^- + H_2O + e^- \quad (1)$$

$$2AgNO_3 + 2e^- \rightarrow 2Ag + O_2 + 2NO_2 \quad (2)$$

$$HAuCl_4 + 3e^- \rightarrow 2Au + 4Cl^- + H^+ \quad (3)$$

Figure S4 in the Supporting Information shows the SPR spectra with maximum absorptions at 476 and 543 nm because of Ag and Au NPs formation. The intensities of both spectra are low, especially for Au NPs compared to that under optimum conditions (Figure 3) mainly because of either larger sized particles or incomplete reduction in the absence of LE. Further, it can be seen that the NPs obtained in the absence of LE are reasonably larger and wider in size distribution and shape (SEM images in Figure S4, Supporting Information) when compared with those obtained in optimum conditions (Figure 5). The particle sizes obtained in the absence of LE are ~40 nm (spherical) for Ag NPs and ~80−700 nm (spherical to irregular sizes) for Au NPs. Thus, we can say that some notable synergism between LE and natural surfactants was playing an influential role in controlling the particles size and distribution.

FT-IR Studies. The FT-IR measurements were carried out to identify the possible biomolecules responsible for stabilization and capping of the formed metal NPs under different conditions. Figure 6 shows spectral patterns of pure LE (a), Acacia (b), Reetha (c), Ag NPs−Acaia (d), and Au NPs−Reetha (e). The FT-IR spectrum of pure LE shows significant absorption bands at 3246, 2931, 1592, 1372, 1065, and peaks in the region 970−650 cm^{-1} (961, 817, 765 cm^{-1}). The observed band pattern for different functional groups as well as fingerprint region of polyphenols present in LE was identified before in our previous study.[7]

The FT-IR spectra of Acacia and Reetha according to Coates[30] are as follows: peaks of hydroxyl group (−OH) at 3346 cm^{-1} (for b) and 3388 cm^{-1} (for c); C—H stretching at 2927 cm^{-1} for both b and c; C═O stretch at ~1700 and 1724 cm^{-1} aere observed for b and c, respectively, because of the presence of aldehyde group; C═C absorption at 1619 cm^{-1} identified for (b); oligosaccharide linkage absorptions to sapogenins of saponins with C—O—C were evident at 1061 cm^{-1} (for b) and 1037 cm^{-1} (for c); 1365 cm^{-1} for b and 1369 cm^{-1} for c are because of methyl group; The peaks at 1006 cm^{-1} of b and 912 cm^{-1} of c are because of cyclohexane ring vibrations of saponins arise due to methylene group; the peak at 1233 cm^{-1} for c is for primary alcoholic $-CH_2OH$ group attached to cyclohexane ring. This group is absent in the saponin structure of Acacia (b).

The FT-IR spectra of water washed Ag and Au NPs in the presence of mixture of natural surfactants and LE using optimum conditions are shown in panels f and g of Figure 6, respectively, and compared with the pure extracts (panels a, b, and c) as well as NPs synthesized using pure saponins (panels d and e). Figure 6d,e shows peaks related to typical saponins for Ag and Au NPs formed from individual Acacia and Reetha and therefore support the capping effect of these surfactants after physical adsorption on the NPs surface in the absence of LE.

In addition to the above, the spectra of Au and Ag NPs formed from the optimum conditions (Figure 6f,g) show both peaks of the used LE and saponins. For example, spectral splitting at around ~1000 cm^{-1} in Figure 6f,g infers the presence of a C−O group of the polyphenol and C−O−C stretch of sapogenins in saponins. It has also been observed that in the mixed system LE peak dominates over the saponin, even after repeated water washings.

Bacterial Sensitivity Tests. The metal NPs such as Ag and Au with smaller sizes have huge scope as a new class of antimicrobial agents and are being used extensively in many bactericidal fields.[31−34] The antimicrobial activity of as synthesized Ag and Au NPs was tested on *E. coli* and the results are presented in SI-II (Supporting Information). The ZOI results show significant antimicrobial property by Ag NPs,

DOI: 10.1021/acssuschemeng.5b00022
ACS Sustainable Chem. Eng. 2015, 3, 483−491

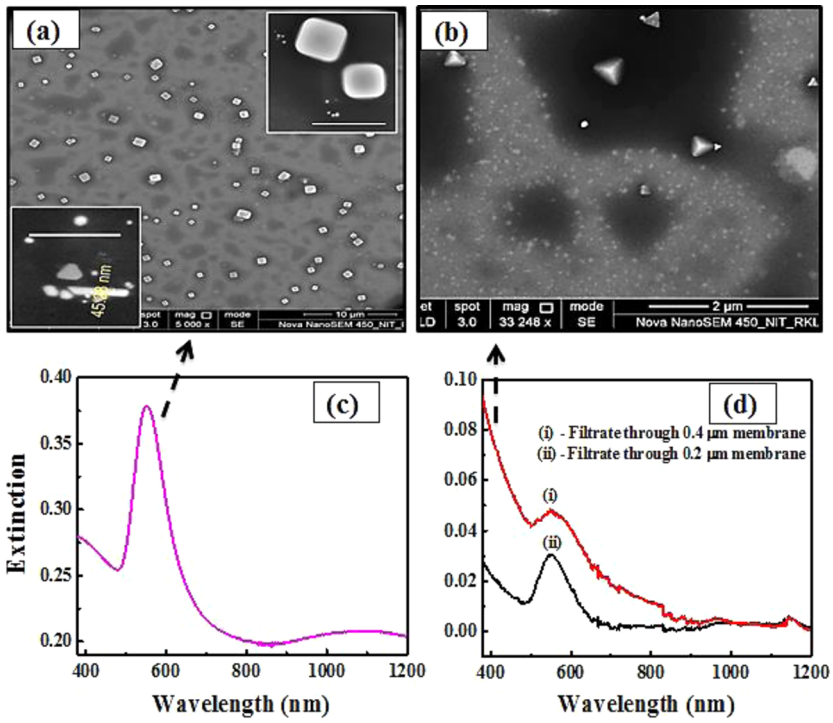

Figure 7. FESEM images of the (a) as-prepared Au NPs with cubes, spheres, and triangular structures; scale bar of the insets is 0.5 μm. Panel b shows only spherical and triangular NPs after separation of Au square nanoplates. Respective UV−visible spectra of the (c) as-prepared and (d) residual NPs after filtration.

whereas the tested *E. coli* was insensitive to Au NPs (Figure S5a,a′-b,b′, Supporting Information) at that dose.

Synthesis of Anisotropic Au Square Nanoplates. It has been shown before that the Taguchi method is useful for designing of optimum parameters to get small sized spherical NPs. After the results of the different trials were analyzed, trial 3, for Au NPs, showed two absorption peaks (551 and 1095 nm) in contrast to other trials (Figure S1, Supporting Information). The different parameters of trial 3 are pH = 5.0, media is Reetha, temperature = 40 °C, blue light, reactant proportion 1/0.3, as mentioned in Table S2 (Supporting Information). The absorption of light in the UV−visible region by the metal NPs is mainly because of SPR phenomenon, which in turn sensitive to the size and shape of the respective NPs. In general, the absorption peak in the NIR region indicates the presence of nonspherical particles, so, to get an idea about the NIR peak position, the as-prepared Au NPs were observed under field emission (FE)SEM for detail morphology. Figure 7a shows the NPs synthesized in trial 3 are a mixture of spherical, cubical, and triangular (pyramidal) shapes. The average edge length size of Au square nanoplates are ∼630 nm with a thickness of ∼45 nm and the particle size distribution from various images are shown in Figure S7 (Supporting Information). The UV−visible spectrum of the as-prepared solution with mixed size/shape NPs is shown in Figure 7c. The changes in the spectral pattern of Au NPs suspension after filtration through 0.4 and 0.2 μm membranes are also displayed in Figure 7d, and the FESEM image of NPs after filtration through 0.4 μm membrane is shown in Figure 7b. The shape dependent spectral and XRD pattern changes are discussed in the Supporting Information, section SI-III. So, this study clearly indicates that same protocol of different proportion can also be used to get different shapes of Au nano-to-colloidal particles.

CONCLUSIONS

Size and shape controlled metal NPs with a uniform size distribution has been attracting enormous academic and practical interest in recent years. Taguchi statistical design is a simple fractional factorial approach and can be used to optimize production conditions of various NPs. In this study, Au and Ag nanoparticles are synthesized using different plant surfactants (saponin) and *Aegle marmelos* leaf extract as reducing agents. The leaf extract alone can successfully reduce; however, the presence of plant surfactants helps to reduce the size further. Because different parameters are involved in the nanoparticles synthesis process, the Taguchi method was used to get further smaller sized spherical Ag (∼13 nm) and nonspherical Au (∼23 nm) NPs by optimizing the parameters. The optimum conditions obtained for Ag (reactant ratio = 1 mM/0.3%, Acacia media, pH = 7.0, temperature = 55 °C, white light) are different than those of Au (reactant ratio = 1 mM/1.0%, Reetha media, pH = 8.5, temperature = 40 °C, dark) NPs. The synergistic effect of the polyphenols of plant extract and natural surfactants (Acacia or Reetha) plays a crucial role in regulating the smaller sized noble metal NPs. Although most of the extinction spectra of Au NPs trials with their SPR mostly lying in the visible region, alteration of the parameters from a particular trial (no. 3) resulted in square nanoplate and pyramidal shape Au NPs with its extinction spectrum extended from visible to NIR region. Because the reported study is a simple, green route, single step one-pot process, it has a huge implications for economical production of metal NPs by reducing trial runs.

DOI: 10.1021/acssuschemeng.5b00022
ACS Sustainable Chem. Eng. 2015, 3, 483−491

■ ASSOCIATED CONTENT

Supporting Information

Experimental details of preparation of saponins, XRD and ζ potential figures of Ag and Au NPs, UV−visible spectra of the Ag and Au NPs synthesized from control experiments, details of bacterial sensitivity tests, L16 array and ANOVA tables of the NPs synthesis. This material is available free of charge via the Internet at http://pubs.acs.org.

■ AUTHOR INFORMATION

Corresponding Author

*S. Paria. E-mail: santanuparia@yahoo.com, or sparia@nitrkl.ac.in. Fax: +91 661 246 2999.

Notes

The authors declare no competing financial interest.

■ REFERENCES

(1) Kharissova, O. V.; Dias, H. V. R.; Kharisov, B. I.; Pérez, B. O.; Pérez, V. M. J. The greener synthesis of nanoparticles. *Trends Biotechnol.* **2013**, *31*, 240−248.
(2) Mittal, A. K.; Chisti, Y.; Banerjee, U. C. Synthesis of metallic nanoparticles using plant extracts. *Biotechnol. Adv.* **2013**, *31*, 346−356.
(3) Brust, M.; Kiely, C. J. Some recent advances in nanostructure preparation from gold and silver particles: A short topical review. *Colloids Surf., A* **2002**, *202*, 175−186.
(4) Clark, J. H. Green chemistry: Challenges and opportunities. *Green Chem.* **1999**, *1*, 1−8.
(5) Jha, A. K.; Prasad, K.; Prasad, K.; Kulkarni, A. R. Plant system: Nature's nanofactory. *Colloids Surf., B* **2009**, *73*, 219−223.
(6) Girija, S.; Balachandran, Y. L.; Kandakumar, J. Plants as green nanofactories: Application of plant biotechnology in nanoparticle synthesis - A review. *Plant Cell Biotechnol. Mol. Biol.* **2009**, *10*, 79−86.
(7) Jagajjanani Rao, K.; Paria, S. Green synthesis of silver nanoparticles from aqueous *Aegle marmelos* leaf extract. *Mater. Res. Bull.* **2013**, *48*, 628−634.
(8) Roy, R. K. *Design of Experiments Using The Taguchi Approach: 16 Steps to Product and Process Improvement*; John Wiley & Sons: New York, 2001.
(9) Chiang, Y. D.; Lian, H. Y.; Leo, S. Y.; Wang, S. G.; Yamauchi, Y.; Wu, K. C.W. Controlling particle size and structural properties of mesoporous silica nanoparticles using the Taguchi method. *J. Phys. Chem. C* **2011**, *115*, 13158−13165.
(10) Kim, K. D.; Kim, S. H.; Kim, H. T. Applying the Taguchi method to the optimization for the synthesis of TiO_2 nanoparticles by hydrolysis of TEOT in micelles. *Colloids Surf., A* **2005**, *254*, 99−105.
(11) Alamdari, R. F.; Hajimirsadeghi, S. S.; Kohsari, I. Synthesis of silver chromate nanoparticles: Parameter optimization using Taguchi design. *Inorg. Mater.* **2010**, *46*, 60−64.
(12) Park, S. K.; Kim, K. D.; Kim, H. T. Preparation of silica nanoparticles: Determination of the optimal synthesis conditions for small and uniform particles. *Colloids Surf., A* **2002**, *197*, 7−17.
(13) Biswal, N. R.; Paria, S. Interfacial and wetting behavior of natural−synthetic mixed surfactant systems. *RSC Adv.* **2014**, *4*, 9182−9188.
(14) Rao, K. J.; Paria, S. Solubilization of naphthalene in the presence of plant−synthetic mixed surfactant systems. *J. Phys. Chem. B* **2009**, *113*, 474−481.
(15) Abul Gafur, M.; Obata, T.; Kiuchi, F.; Tsuda, Y. *Acacia concinna* saponins. I. Structures of prosapogenols, concinnosides A-F, isolated from the alkaline hydrolysate of the highly polar saponin fraction. *Chem. Pharm. Bull. (Tokyo)* **1997**, *45*, 620−625.
(16) Tezuka, Y.; Honda, K.; Banskota, A. H.; Thet, M. M.; Kadota, S. Kinmoonosides A−C, Three new cytotoxic saponins from the fruits of *Acacia concinna*, a medicinal plant collected in Myanmar. *J. Nat. Prod.* **2000**, *63*, 1658−1664.
(17) Mahato, S. B.; Pal, B. C.; Nandy, A. K. Structure elucidation of two acylated triterpenoid bisglycosides from *Acacia auriculiformis* cunn. *Tetrahedron* **1992**, *48*, 6717−6728.
(18) Majhi, P. R.; Mukherjee, K.; Moulik, S. P.; Sen, S.; Sahu, N. P. Solution properties of a saponin (Acaciaside) in the presence of Triton X-100 and Igepal. *Langmuir* **1999**, *15*, 6624−6630.
(19) Nanda, A.; Saravanan, M. Biosynthesis of silver nanoparticles from *Staphylococcus aureus* and its antimicrobial activity against MRSA and MRSE. *Nanomed.: Nanotechnol., Biol. Med.* **2009**, *5*, 452−456.
(20) Kalishwaralal, K.; Deepak, V.; Ramkumarpandian, S.; Nellaiah, H.; Sangiliyandi, G. Extracellular biosynthesis of silver nanoparticles by the culture supernatant of *Bacillus licheniformis*. *Mater. Lett.* **2008**, *62*, 4411−4413.
(21) Sadowski, Z. Biosynthesis and application of silver and gold nanoparticles. *Silver Nanoparticles* **2010**, 257−276.
(22) Birla, S. S.; Gaikwad, S. C.; Gade, A. K.; Rai, M. K. Rapid synthesis of silver nanoparticles from *Fusarium oxysporum* by optimizing physicocultural conditions. *Sci. World J.* **2013**, *2013*, 1−12.
(23) Jain, P. K.; Huang, X.; El-Sayed, I. H.; El-Sayed, M. A. Review of some interesting surface plasmon resonance-enhanced properties of noble metal nanoparticles and their applications to biosystems. *Plasmonics* **2007**, *2*, 107−118.
(24) Azin, M.; Moravej, R.; Zareh, D. Production of xylanase by *Trichoderma longibrachiatum* on a mixture of wheat bran and wheat straw: Optimization of culture condition by Taguchi method. *Enzyme Microb. Technol.* **2007**, *40*, 801−805.
(25) Sajanlal, P. R.; Sreeprasad, T. S.; Samal, A. K.; Pradeep, T. Anisotropic nanomaterials: Structure, growth, assembly, and functions. *Nano Rev.* **2011**, *2*.
(26) Dahl, J. A.; Maddux, B. L. S.; Hutchison, J. E. Toward greener nanosynthesis. *Chem. Rev.* **2007**, *107*, 2228−2269.
(27) Patra, H. K.; Banerjee, S.; Chaudhuri, U.; Lahiri, P.; Dasgupta, A. K. Cell selective response to gold nanoparticles. *Nanomed: Nanotechnol., Biol. Med.* **2007**, *3*, 111−119.
(28) Elavazhagan, T.; Arunachalam, K. D. Memecylon edule leaf extract mediated green synthesis of silver and gold nanoparticles. *Int. J. Nanomed.* **2011**, *6*, 1265−1278.
(29) Shankar, S. S.; Rai, A.; Ahmad, A.; Sastry, M. Rapid synthesis of Au, Ag, and bimetallic Au core-Ag shell nanoparticles using neem (*Azadirachta indica*) leaf broth. *J. Colloid Interface Sci.* **2004**, *275*, 496−502.
(30) Coates, J. *Interpretation of Infrared Spectra, A Practical Approach*; Wiley Online Library: New York, 2000.
(31) Zhang, Y.; Peng, H.; Huang, W.; Zhou, Y.; Yan, D. Facile preparation and characterization of highly antimicrobial colloid Ag or Au nanoparticles. *J. Colloid Interface Sci.* **2008**, *325*, 371−376.
(32) Li, Q.; Mahendra, S.; Lyon, D. Y.; Brunet, L.; Liga, M. V.; Li, D.; Alvarez, P. J. J. Antimicrobial nanomaterials for water disinfection and microbial control: Potential applications and implications. *Water Res.* **2008**, *42*, 4591−4602.
(33) Chaloupka, K.; Malam, Y.; Seifalian, A. M. Nanosilver as a new generation of nanoproduct in biomedical applications. *Trends Biotechnol.* **2010**, *28*, 580−588.
(34) Sharma, V. K.; Yngard, R. a; Lin, Y. Silver nanoparticles: Green synthesis and their antimicrobial activities. *Adv. Colloid Interface Sci.* **2009**, *145*, 83−96.

DOI: 10.1021/acssuschemeng.5b00022
ACS Sustainable Chem. Eng. 2015, 3, 483−491